Letters

*Determination of the surface residual stresses in tempered glasses by indentation fracture mechanics**

It is well known that the extent of surface cracking about the corners of a Vickers pyramid indentation reflects the fracture toughness and the state of surface stresses of materials [1–4]. The advantages of this approach of characterizing materials and determining surface stresses are

(i) many tests may be performed on a small sample not necessarily suitable for optical assessment of the residual stresses;

(ii) fracture toughness may be obtained on samples not suitable for conventional testing techniques;

(iii) the observations are not unduly influenced by pre-existing surface flaw distribution;

(iv) the simplicity and ease of this test. However until recently it has been difficult to use these observations to precisely quantify either the fracture toughness or the residual surface stresses.

For transparent materials there are a number of approaches to measure the residual stresses after tempering. These include optical techniques (laser interference and stress birefringence for transparent materials [5], fracturing in flexure [6], and indentation fracture with spherical indenters [7]. All of these techniques have associated problems such as refractive effects near the surface, edge failure, and significant influence of the surface flaw distribution respectively.

Recently Lawn and Fuller [8] have provided a fracture mechanics basis to the approach first outlined by Palmqvist [1]. This has enabled fracture toughness determinations to be made from simple pointed indentation tests which are in good agreement with other methods of fracture toughness analysis.

Beneath a pointed indenter under load a penny-shaped crack is observed to form which on unloading extends to the surface. In the case of a Vickers pyramid the extension is primarily directed along the corners of the remnant impression [9]. The crack grows stably with load and retains its penny shape. The stress intensity factor at the crack tip K_p is given by [8]

$$K_p = \frac{XP}{c^{3/2}} \quad (1)$$

where $2c$ is the crack diameter, P is the indenter load and X is a geometric factor determined by the indenter geometry and is given by

$$X = 1/\tan \psi \pi^{3/2},$$

and ψ is the half-angle of the indenter. When there is friction between the indenter and specimen then ψ may be replaced by $\psi + \tan^{-1}\mu$, where μ is the coefficient of friction.

Lawn and Fuller [8] also observed that the extent of the surface traces about pointed indenters mirrored the subsurface behaviour, except that the surface trace diameter was approximately twice the subsurface depth of the cracks. These surface traces often formed on unloading and hence they owe their existence to the residual stresses about the permanent hardness impression. Unfortunately our knowledge of the magnitude and distribution of the residual stresses is limited at present although a recent estimate of the maginitude of these stresses from fracture mechanics observations suggests a value of $H/20$ [10]. Despite these limitations further observations by Lawn *et al.* [11] confirmed that Equation 1 held for surface traces about a Vickers hardness impression. These same authors used this approach to determine the minimum load to propagate cracks about the indentation site.

For the case of materials with surface compressive or tensile stresses, the stress intensity factor for a two dimensional crack of length $2c$ subjected to this stress is given by [12]

$$K_c = \bar{\sigma}_R \sqrt{c}, \quad (2)$$

where $\bar{\sigma}_R$ is the mean stress over the crack. For tempered glasses and ceramics the compressive stresses vary in a systematic manner with depth depending upon the tempering process. A more

* A somewhat similar analysis has recently been published; D. B. MARSHALL and B. R. LAWN, *J. Amer. Ceram. Soc.* **60** (1977) 86.

complete description of this aspect of tempered glasses has been given by Lawn and Marshall [13]. Now from the additive property of the stresses, the stress intensity factor at the tip of a crack created during a pointed indentation test on a tempered material is, from Equations 1 and 2 given by

$$K_{eq} = K_p + K_c \quad (3)$$

where K_{eq} is the equilibrium value of the stress intensity factor for the untempered material under the environmental conditions tested. From Equation 3 upon substituting for K_p and K_c and rearranging, we get

$$\frac{\bar{\sigma}_R}{X} = \frac{P - P'}{c^2}. \quad (4)$$

It is now a simple matter to determine $\bar{\sigma}_R$ from a plot of $P - P'$ against c^2, where P' is the indenter load to form a crack of length $2c$ on the surface of the tempered glass.

Tests were carried out on a number of commercially available thermally tempered glasses. Indentations were performed using a heavy duty Vickers diamond pyramid with a Leitz microhardness tester, for loads less than 20 N, and on an Instron testing machine. The surface traces of the cracks about the indentation site were measured in transmission microscopy ~1 h after the load was removed.

TABLE I

Material	Residual Stress from Indentation (MPa)	Residual Stress Manufacturers' Value (MPa)
Thermally tempered Glass A	220	~ 210
Thermally tempered Glass B	103	~ 140
Thermally tempered Glass C	64	~ 52

The values of the residual stresses were obtained using Equation 4 from plots of $P - P'$ against c^2, as shown in Fig. 1. The results of the residual stresses are listed in Table I along with the suppliers' nominal values for the residual stresses. The agreement between the two sets of observations is quite good.

One other interesting point emerges from the present work: the influence of the residual stress on the indentation load to propagate a crack about the indentation site. Following Lawn *et al.* [11] the diagonal of the impression $2a$ and diameter of

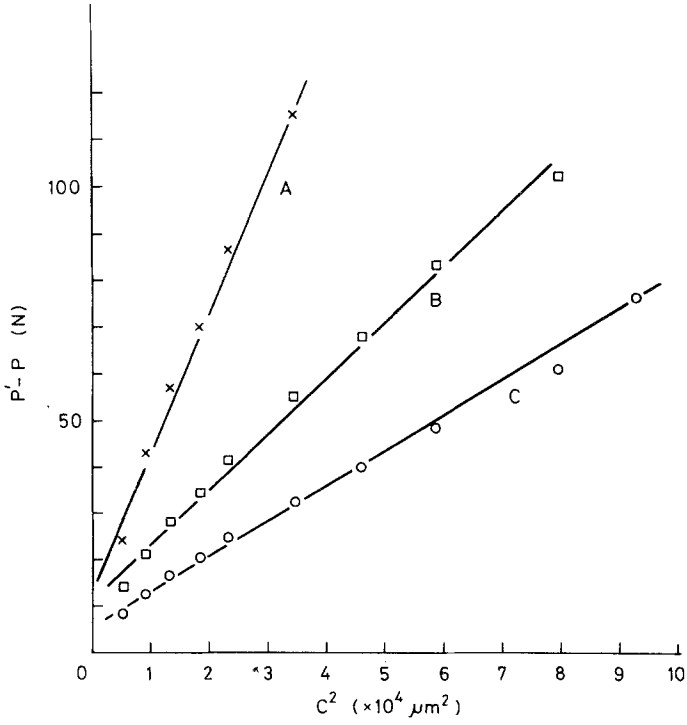

Figure 1 A plot of $P' - P$ against c^2 for three thermally tempered soda-lime silicate glasses.

the surface trace of the crack $2c$ are plotted against the indenter load for the glasses studied, Fig. 2. The diagonal of contact $2a$ varied very little with glass treatment and hence only one curve is shown in Fig. 2. The intersection of the crack diameter and contact diagonal indicates the critical indentation load to form a flaw in a particular tempered glass. This observation is consistent with other work [15] which noted that unless a flaw is visible outside the diameter of contact then no strength degradation of tempered glasses is observed.

Although the analysis above is only applicable for the propagation of developed cracks it is possible to predict approximately the load required on an indenter to initiate a crack greater than the relationship between hardness, load and contact diameter of contact. From Equation 1 and the diagonal for Vickers pyramid

$$a^2 = \frac{P}{2H} \tag{5}$$

then the threshold indentation half-diagonal for annealed glass is

$$a_c = \left[\frac{K_{eq}}{2XH}\right]^2 \tag{6}$$

and for tempered glasses from Equations 2, 3 and 6 we have

$$a_c = \left[\frac{K_{eq}}{2XH + \bar{\sigma}_R}\right]^2 \tag{7}$$

Upon substituting for K_{eq} and the measured or known values of $\bar{\sigma}_R$ the critical indentation diagonal and hence load may be found. Tests were carried out on a thermally tempered sample of aluminosilicate glass to check Equation 7. The hardness, equilibrium stress intensity factor and residual stress of the aluminosilicate were known to be 7×10^9 Pa, 8×10^5 N m$^{-3/2}$ [14] and 80 MPa [16] respectively. Upon substituting in Equations 7 and 6 the critical load initiate fracture is 0.15 N and experiments indicated that it occurred between 0.5 and 1.0 N, which is reasonable considering the simplicity of the model and the approximations made.

The application of simple fracture mechanics principles has enabled the residual stress resulting from some tempering process to be determined from indentation tests. The determination of the residual stress, although a mean of the stress over the region in which the crack finds itself, is in good agreement with optical techniques. This tech-

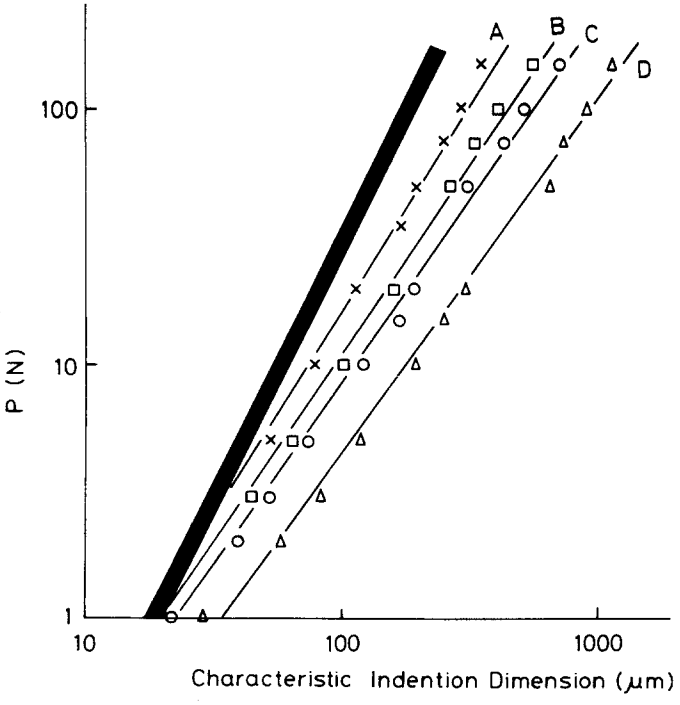

Figure 2 Characteristic indentation dimension, $2a$ (heavy line) and $2c$, for the three thermally tempered glasses and annealed soda-lime glass (D) as a function of indenter load with a Vickers pyramid.

nique has many advantages over others in that it requires the minimum of sophistication and sample preparation and does not require a transparent material.

This method also enables a conservative estimate of the critical load to form strength reducing flaws in tempered materials. This last point should be of considerable interest for the prediction of the resistance of a particular tempering to the initiation of flaws owing to scratching, grinding, indenting or impacting with sharp objects.

Acknowledgements

The S.R.C. is thanked for financial support and the M.O.D. (P.E.) for a grant to the laboratory.

References

1. S. PALMQVIST, *Jernkontorets Ann.* **141** (1971) 300.
2. *Idem, Arch. Eisenhuettenw* **33** (1962) 629.
3. W. DAWIHL and G. ALTMEYER, *Z. Mettalk.* **55** (1962) 231.
4. H. E. EXNER, *Trans. Met. Soc. AIME* **245** (1969) 677.
5. A. KUSKE and G. ROBERTSON, "Photoelastic Analysis" (Wiley, London, 1974) Chapter 16.
6. J. T. HAGAN, M. V. SWAIN and J. E. FIELD, *Glass Technol.* (in press).
7. B. R. LAWN and T. R. WILSHAW, *J. Mater. Sci.* **10** (1975) 1049.
8. B. R. LAWN and E. R. FULLER, *ibid* **10** (1975) 2016.
9. B. R. LAWN and M. V. SWAIN, *ibid* **10** (1975) 113.
10. M. V. SWAIN, *ibid* **11** (1976) 2345.
11. B. R. LAWN, T. JENSEN and A. ARORA, *ibid* **11** (1976) 573.
12. G. C. SIH, "Handbook of Stress Intensity Factors', (Lehigh University, Bethelehem, U.S.A. 1973).
13. B. R. LAWN and D. B. MARSHALL, *Phys. Chem. Glasses* **18** (1977) 7.
14. S. M. WIEDERHORN, *J. Amer. Ceram. Soc.* **52** (1969) 99.
15. M. V. SWAIN and J. T. HAGAN, unpublished work.
16. A. WOODWARD, private communication (1976).

Received 14 January
and Accepted 18 Feberuary 1977.

M. V. SWAIN,
J. T. HAGAN,
J. E. FIELD
Physics and Chemistry of Solids Section,
Cavendish Laboratory,
Madingley Road,
Cambridge, UK

Cavity formation at grain boundary–sub-boundary intersections in pure α-iron and an iron 0.14 wt % phosphorus alloy

It is well established that grain boundary cavities nucleated during creep do so at heterogeneous sites which are either "grown in" or produced during the creep deformation process. The mechanisms and processes suggested for cavity nucleation have been recently reviewed by Perry [1]. Some recent direct observations of cavity formation in α-iron [2] and copper alloys [3] have shown that particles located on grain boundaries are preferential sites for cavities.

This note is concerned with the behaviour of α-iron and an iron–0.14 wt % phosphorus alloy which contained a very low volume fraction of particles. The presence of the phosphorus resulted in enhanced low-temperature (−196° C) grain-boundary embrittlement and as a consequence, cavities formed during creep deformation could be

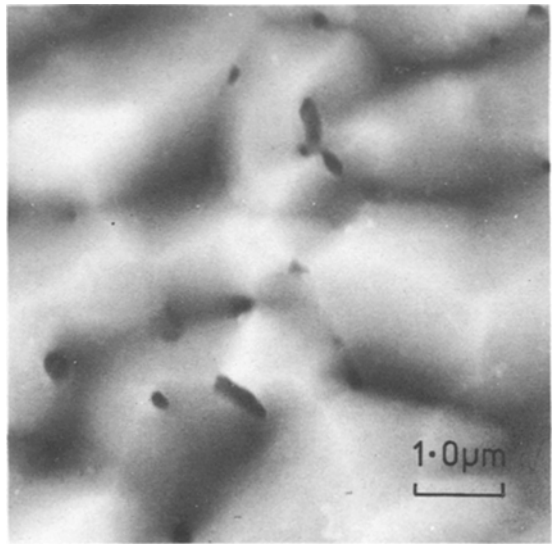

Figure 1 Sub-micron cavities and cell structure in Fe–0.14 wt % P after 21.2% creep strain at 423° C.